

# HIGH RESOLUTION FLEXIBLE STRAIN SENSORS FOR BIOLOGICAL SIGNAL MEASUREMENTS

Yichuan Wu<sup>1,2</sup>, Levent Beker<sup>2</sup>, Ilbey Karakurt<sup>2</sup>, Weihua Cai<sup>2,3</sup>, Jacqueline Elwood<sup>2</sup>, Xiaoqian Li<sup>2,4</sup>, Junwen Zhong<sup>2</sup>, Min Zhang<sup>5\*</sup>, Xiaohao Wang<sup>1,5\*</sup>, and Liwei Lin<sup>1,2\*</sup>

<sup>1</sup>Tsinghua-Berkeley Shenzhen Institute, Tsinghua University, CHINA

<sup>2</sup>University of California, Berkeley, USA

<sup>3</sup>South China University of Technology, CHINA

<sup>4</sup>Southeast University, CHINA

<sup>5</sup>Graduate School at Shenzhen, Tsinghua University, CHINA

## ABSTRACT

This paper presents stretchable strain sensors based on Polydimethylsiloxane (PDMS)/graphite sensing resistors for potentially a variety of wearable device applications including human biological signal measurements, such as fingertip pressure monitoring for haptic feedback and high resolution arterial pulse for health diagnostics. The strain sensor uses a serpentine electrode design that can be easily fabricated in a two-step process by direct-write laser printing and pattern transfer without any lithography process. The results demonstrate several key sensing capabilities: (1) angular motion detection with a resolution of 15-degree; (2) fingertip pressure detection up to a range of 12 kPa; (3) monitoring of human pulse waves with the clear identification of the three local peaks. As such, the proposed strain sensors can be potentially used as a biological signal input device for potential applications such in virtual reality (VR) systems.

## KEYWORDS

PDMS; graphite; strain sensor; wearable device; piezoresistive

## INTRODUCTION

Flexible electronic devices have received great attentions in recent years because of their potential uses in various fields ranging from entertainment, medicine, to wearable consumer electronics [1-2]. For example, tactile sensors, or commonly referred as arrays of strain and/or pressure sensors, can collect physical interactions with environment [3]. However, the functions and resolutions of state-of-art tactile sensors are limited with difficulties in detecting finger/hand motions, fingertip pressure, and arterial pulse waves for various possible applications. For example, some of the current methods can only provide discrete inputs, whereas continuous monitoring is highly desired in many applications. Previously, stretchable strain/pressure sensors have been constructed by using carbon nanotubes, silver nanowires, graphene, and polymer nanofibers for wearable systems [4-10]. However, they usually require complex fabrication processes with small piezoresistive gauge factors. Yang *et al.* have shown an arterial pulse wave sensor that uses a complex fabrication process based on piezoelectric materials [11]. Lin *et al.* have reported a one-step approach for producing and patterning porous graphene films from commercial polymer films using a CO<sub>2</sub> infrared laser for rapid constructions of flexible electrodes [12]. Based on this laser induced graphite

technique, many flexible devices such as supercapacitors [13], UV sensors [14] and strain sensors [15] have been reported. Specifically, Rahimi *et al.* have proposed a simple and cost effective fabrication process based on PDMS/graphite materials using laser induced graphite [16]. However, a high precision/resolution wearable sensing system for applications such as fingertip pressure and arterial pulse waves has not been demonstrated. Here, we report a thin film PDMS/graphite-based stretchable strain sensor for a variety of wearable device applications including biological signal measurements, such as to monitor continuous finger motions, fingertip pressure, and arterial pulse waves with high resolution.

## CONCEPT & PRINCIPLE

VR applications using head-mounted sets are popular in the video game industry, military usages and medical trainings. The visible images and video clips coupled with sound effects generated by the VR systems are intended to emulate a real environment and tactile systems can be added to generate force feedback in creating more realistic sensations. For example, some of the current VR systems use voice commands and physical tools with physical buttons (e.g., Oculus Rift's touch) as force feedback for the human machine interfaces. However, they lack the ability to convey realistic tactile sensations based on bulky devices, which are not stretchable with limited resolutions.

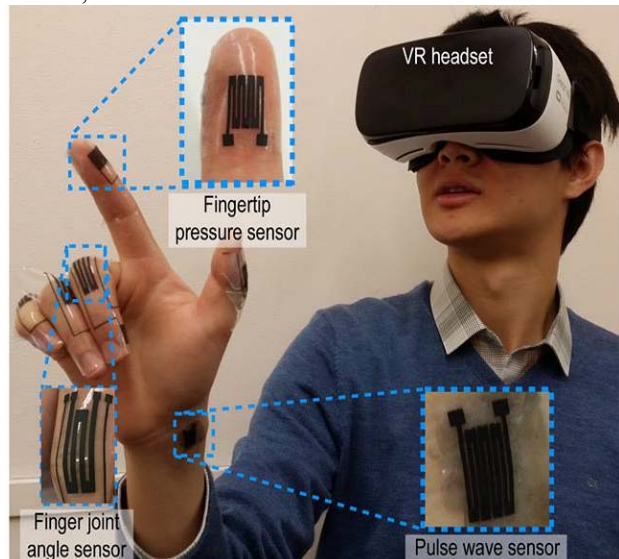


Fig. 1: The proposed wearable strain sensors together with a head mounted VR system to illustrate the potential applications.

Figure 1 conceptually depicts the proposed biological signal measurement system implanted to a VR system, which can potentially give the biological signal feedback, such as finger gesture motion recognitions, fingertip pressure sensing, and human pulse waves monitoring. All the targeted biological signals are collected by the thin flexible strain sensors which are conformed to human body. The flexible strain sensors are based on the principle of the piezoresistive effect. Under a certain strain or deformation, the strain sensors can cause the resistance change which can be detected by outside circuits.

## FABRICATION PROCESS

For the finger-joint bending sensors and fingertip pressure sensors, we utilize the serpentine sensing structures as the sensing electrodes as shown in Figure 2. The serpentine structure helps increasing the sensitivity along the length direction of the sensor under a fixed strain because it has a longer material path in the sensing direction with the minimum occupation of the whole sensing area. In the serpentine structure, each single line is in series connected. The resistance change, which is caused by any strain of a single piece, can be added together so that they will make accumulative contributions to improve the sensitivity of the system.

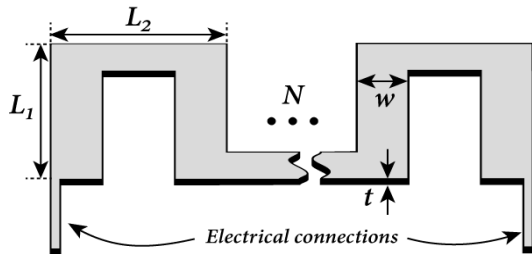


Fig. 2: Schematic diagram showing the design pattern of the strain sensing structure.

The main parameters, such as the numbers of serpentine structures, length, width of each cycle and the working range of resistance, have been designed with the specific values as listed in Table 1 in our prototype. For the finger-joint sensor, we chose 3 cycles of serpentine structure with larger length and width to accommodate a large range of the potential strain range as caused by the bending of the finger. On the other hand, for the fingertip pressure sensor, high sensitivity is the first priority such that the 8-cycle serpentine structure design with smaller length and width is chosen as more cycles and smaller electrode width can improve the sensitivity. Finally, the resistance changes of finger-joint sensor are measured after the prototype fabrication process as from  $9\text{k}\Omega$  to  $595\text{k}\Omega$  and the fingertip pressure sensor is from  $15\text{k}\Omega$  to  $200\text{k}\Omega$ .

Table 1 Prototype sensor design parameters

|       | Finger joint sensor                     | Pressure sensor                          |
|-------|-----------------------------------------|------------------------------------------|
| $N$   | 3cycles                                 | 8cycles                                  |
| $L_1$ | 15mm                                    | 15mm                                     |
| $L_2$ | 5mm                                     | 1.5mm                                    |
| $t$   | $8\mu\text{m}$                          | $8\mu\text{m}$                           |
| $w$   | 2mm                                     | 0.5mm                                    |
| $R$   | $9\text{k}\Omega$ - $595\text{k}\Omega$ | $15\text{k}\Omega$ - $200\text{k}\Omega$ |

Figure 3 (a) shows the basic fabrication process of the strain sensors. First, a  $50\mu\text{m}$ -thick commercial polyimide (PI) tape is attached to a silicon wafer, which serves as a large, flat, and heat conductive substrate. Laser-induced porous graphite structures are patterned by the direct writing of  $\text{CO}_2$  laser on the PI film. The uncured PDMS (Sylgard 184, mixed ratio 10:1) is poured onto the patterned sample and the air is evacuated by a vacuum pump to allow PDMS to fill up the pores in the patterned graphite structures. The thickness of the PDMS film can be controlled according the amount of poured PDMS. The thinner the PDMS substrate is, the more sensitive the strain sensor will be. After curing in the oven at  $60^\circ\text{C}$  for 2 hours, the serpentine-structured strain sensor can be peeled off by hand from the commercial PI tape and the laser-induced graphite layer can be transferred onto the PDMS film. Finally, to protect the porous graphite pattern from peeling off when making contact with an object, the whole structure can be sealed with another thin PDMS layer.

The laser power is one of the most important parameters in the process to induce the porous graphite structures without undesirable ablation on the thin PI film. The carbonization process of the PI film under the laser irradiation is mostly likely by a photothermal mechanism, owing to the long wavelength ( $\sim 10.6\mu\text{m}$ ) and relatively long pulses ( $\sim 14\mu\text{s}$ ) of the  $\text{CO}_2$  laser [12, 17]. The PI film absorbs the incident laser energy and converts it into heat to induce extremely high temperature in the irradiated region to result in carbonization [15]. Some chemical bonds inside the PI film, such as the C—O, C=O and N—C bonds could be easily broken under this high temperature [12]. The thickness of laser induced graphite is estimated by measuring their converted depths in the PI tape using a surface profilometry as shown in Figure 3(b). The laser head scanning speed is fixed at 250mm/s in our process and its power varies from 4.5W to 8.0W to result in the average depth of the graphite layer as 5 to  $30\mu\text{m}$ .

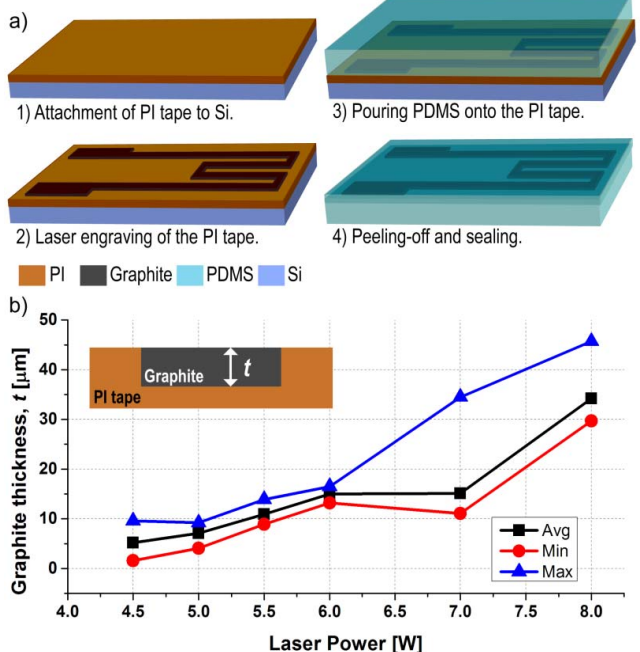


Fig. 3: (a) The fabrication process flow; (b) laser power versus graphite thickness indicating avg., min. and max. depth as measured in fabricated electrodes.

Figure 4 shows the laser-induced patterns with a SEM image exhibiting the porous morphology of the graphite. The carbonized and porous structure contains multilayer graphene flakes [16]. The porous structures are filled by the poured PDMS and after the curing process, these flakes of around 10  $\mu\text{m}$  in diameter are bonded together by PDMS to be still in contact with each other. Under an applied external strain or stress, cracks and slides will occur in the graphite flakes or between their boundaries to result in the changes of the contact areas among the porous graphite structures. More cracks and slides with larger gaps are generated under higher strain to cause larger resistance changes.

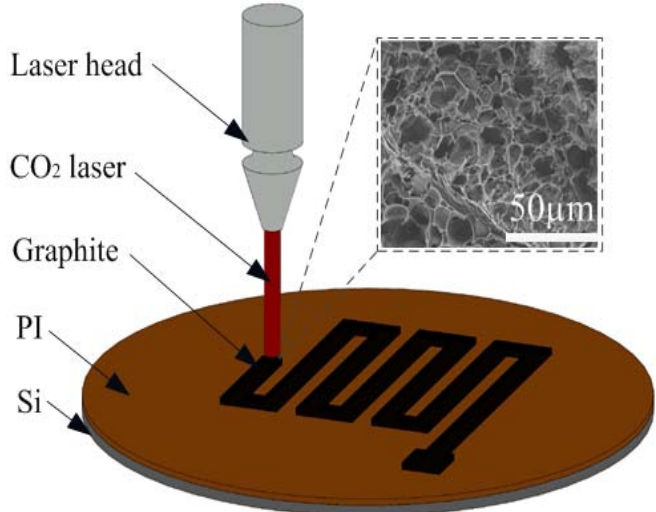


Fig. 4: The serpentine graphite patterns as induced by the direct-write laser patterning process.

## EXPERIMENTAL RESULTS

Figure 5 shows a 3D-printed setup structure to characterize the resistance changes under various bending radii to mimic real applications (e.g. wrist-worn devices). The strain sensor is attached on the surface of the setup structure with different bend radii of 1.0, 1.5, 2.0 and 2.5cm. Results show resistance changes of about 400% for the 1.0cm in radius surface as compared with a flat state.

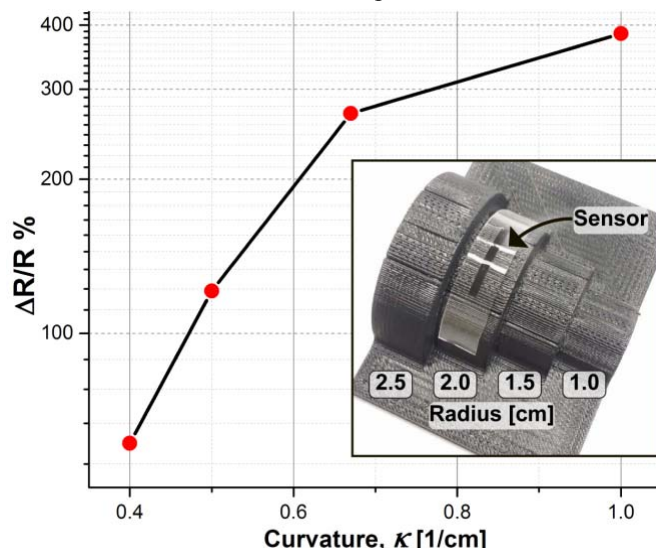


Fig. 5: Resistance changes with respect to the bending curvatures.

When measuring finger-joint bending angles, the thin film strain sensors are attached onto five fingers joints. The two ends of the strain sensors are connected to a potentiometer (GAMRY Instrument, Reference 600). A constant current of 10  $\mu\text{A}$  is applied to the strain sensor. The potential difference can be monitored as the resistance of the strain sensor varies under a certain strain. For monitoring the fingertip pressure, the thin film pressure sensor is mounted on the index fingertip, the resistance of the pressure sensor is measured from a resistance meter (Agilent 34401A) and the force generated by the fingertip is measured by a load cell and the pressure can be approximated by the weight and contact area.

Figure 6 shows the results for the bending angle and pressure tests. A 15-degree discrete increment is clearly monitored in a continuous fashion to demonstrate the continuous monitoring capability in Figure 6(a). The finger joint bending sensor also shows good recovery capability even after going through a 90-degree bending test which is an indication of reliability of the sensor. Figure 6 (b) shows that a pressure sensor is attached to the fingertip of the index finger. The boundaries of the 200  $\mu\text{m}$  thick thin film strain sensor are barely visible. The plot indicates the fingertip pressure sensing can detect from 0 to 12 kPa.

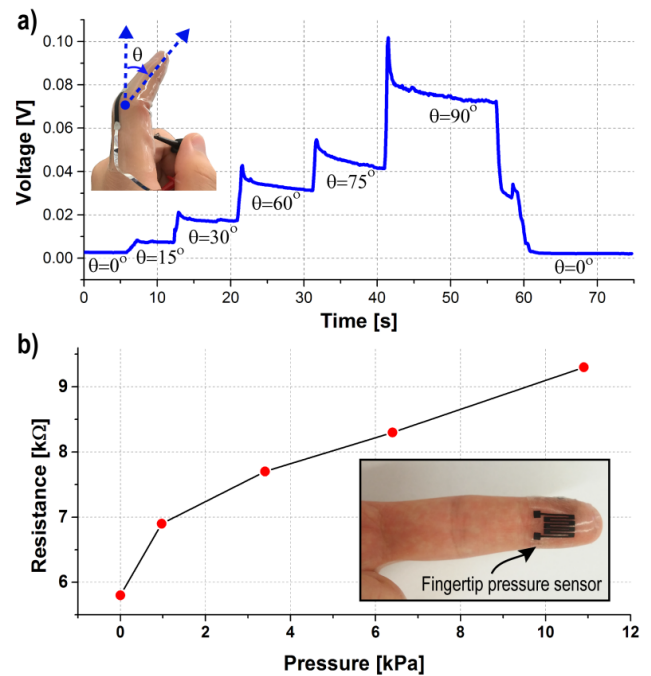


Fig. 5: (a) Continuous finger bending angle experiment; (b) fingertip pressure experiment.

For the arterial pulse measurement, the strain sensor is attached on a wrist. The center of the serpentine structure should be placed on the radial artery where there is a relatively strong beating pulse signal on the wrist in order to record the data. Two ends of the serpentine structure are connected to the GAMRY Instrument and a constant current of 10  $\mu\text{A}$  is applied to the strain sensor.

Figure 7 displays the measurement results of an arterial pulse waveform for 8 seconds and a close-up view of one cycle. It is found that the three peaks of a pulse, systolic (Ps), inflection (Pi) and dicrotic peak (Pd) can be clearly identified. The dicrotic peak (Pd) is known to be

the result of the reflected pulse waves from the lower extremities and aorta. The arterial waveform, which modern physicians have paid little attention, can be significantly affected by the physiological conditions of the human cardiovascular system for possible future applications in medical diagnostic systems.

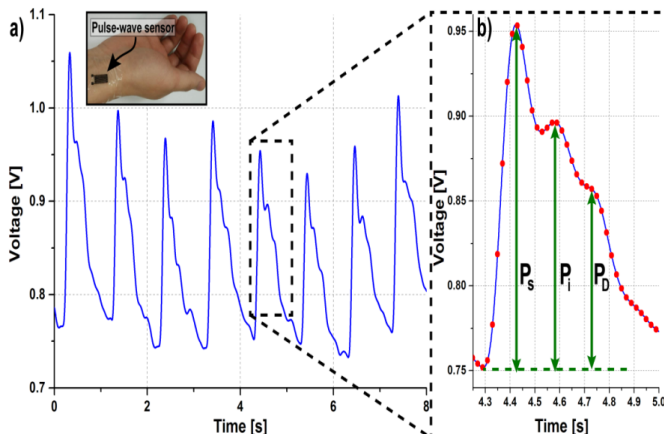


Figure 7: (a) The measured arterial pulse wave for 8 seconds; (b) a close-up view of one cycle showing 3 peaks: systolic ( $P_s$ ), inflection ( $P_i$ ), dicrotic ( $P_d$ ) peaks.

## CONCLUSION

In this work, we demonstrated a highly sensitive flexible strain sensor for biological signal measurements, such as finger-joint bending, fingertip pressing and arterial pulse monitoring by using the direct-write laser patterning and transfer process. The stretchable piezoresistive strain sensors have a total thickness of 200 $\mu$ m, which can be comfortably attached to our hands and joints. We have also investigated the relationship between the laser power and the thickness of laser-induced graphite structures. In order to improve the sensitivity of strain sensors, a serpentine pattern was designed and the optimal design parameters, such as length and width, were characterized in both the finger-joint sensor and the pressure sensor.

## ACKNOWLEDGEMENTS

This work is supported in part by the Berkeley Sensor and actuator Center (BSAC), an NSF/Industry/University Research Cooperation Center. Mr. Y. Wu is supported by a scholarship from the China Scholarship Council (CSC) and Tsinghua-Berkeley Shenzhen Institute (TBSI). The authors also acknowledge the support from the Shenzhen Fundamental Research Funds (JCYJ20150831192244849) and the grant from Guangdong Technology Plan Project (2013B060100008).

## REFERENCES

- [1] A. Chortos et al., "Pursing Prosthetic Electronic Skin," *Nat. Mater.*, Vol. 16, pp. 937-950, 2016
- [2] T. Q. Trung et al., "Flexible and Stretchable Physical Sensor Integrated Platforms for Wearable Human-Activity Monitoring and Personal Healthcare," *Adv. Mater.*, Vol. 28, pp. 4338-4372, 2016.
- [3] T. Yang et al., "Recent Advances in Wearable Tactile Sensors: Materials, Sensing Mechanisms, and Device Performance," *Mater. Sci. Eng. R.*, Vol. 115, pp. 1-37, 2017.
- [4] D. J. Lipomi et al., "Skin-like Pressure and Strain Sensors Based on Transparent Elastic Films of Carbon Nanotubes," *Nat. Nanotechnol.*, Vol. 6, pp. 788-792, 2011.
- [5] T. Yamada et al., "A Stretchable Carbon Nanotube Strain Sensor for Human-motion Detection," *Nat. Nanotechnol.*, Vol. 6, pp. 296-301, 2011.
- [6] J. Shi, et al., "Graphene Reinforced Carbon Nanotube Networks for Wearable Strain Sensors," *Adv. Funct. Mater.*, Vol. 26, pp. 2078-2085, 2016.
- [7] Y. Joo et al., "Silver Nanowire-embedded PDMS with a Multiscale Structure for a highly Sensitive and Robust Flexible Pressure Sensor," *Nanoscale*, Vol. 7, pp. 6208-6215, 2015.
- [8] M. Zhang et al., "All-transparent Graphene-based Flexible Pressure Sensor Array," *Int. J. Mod. Phys. B*, Vol. 31, 2017.
- [9] Y. Pang et al., "Flexible, Highly Sensitive, and Wearable Pressure and Strain Sensors with Graphene Porous Network Structure," *ACS Appl. Mater. Interfaces*, Vol. 8, pp. 26458-26462, 2016.
- [10] C. Shen et al., "Direct-write Polymeric Strain Sensors with Arbitrary Contours on Flexible Substrates," *Proceedings of 29th IEEE MEMS*, pp. 869-872, Shanghai, China, 2016.
- [11] J. Yang et al., "Eardrum - Inspired Active Sensors for Self - Powered Cardiovascular System Characterization and Throat - Attached Anti - Interference Voice Recognition," *Adv. Mater.*, Vol. 27, pp. 1316-1326, 2015.
- [12] J. Lin et al., "Laser-induced porous graphene films from commercial polymers," *Nat. Commun.*, Vol. 5, 2014.
- [13] A. Lamberti et al., "A Highly Stretchable Supercapacitor Using Laser-Induced Graphene Electrodes onto Elastomeric Substrate," *Adv. Energy Mater.*, Vol. 6, (2016).
- [14] D. Wen et al., "Memorizing UV Exposure Energy in Resistance- a Smart Patch Based on Conductive Polymer," *Transducers 2017 Conference*, Kaohsiung, Taiwan, June 18-22, 2017, In Press.
- [15] S. Luo et al., "Direct laser writing for creating porous graphitic structures and their use for flexible and highly sensitive sensor and sensor arrays," *Carbon*, Vol. 96, pp. 522-531, 2016.
- [16] R. Rahimi et al., "Highly Stretchable and Sensitive Unidirectional Strain Sensor via Laser Carbonization," *ACS Appl. Mater. Interfaces*, Vol. 7, pp. 4463-4470, 2015.
- [17] R. Srinivasan et al., "Ultraviolet Laser Ablation of Polyimide Films," *J. Appl. Phys.*, Vol. 61, pp. 372-376, 1987.

## CONTACT

\*e-mail: zhang.min@sz.tsinghua.edu.cn (M. Zhang)  
wang.xiaohao@sz.tsinghua.edu.cn (X. Wang)  
lwlin@berkeley.edu (L. Lin)